

1 Persistent hepatitis B virus and HIV coinfections in dually humanized mice

2 engrafted with human liver and immune system

3 Glenn Hogan^{1,^}, Benjamin Y. Winer^{1,*^}, James Ahodantin^{2,3,^}, Julie Sellau¹, Tiffany
4 Huang¹, Florian Douam^{1,**}, Masaya Funaki^{2,3,***}, Luis Chiriboga⁴, Lishan Su^{2,3,#},
5 Alexander Ploss^{1,#}

1 Department of Molecular Biology, Princeton University, Lewis Thomas Laboratory,
2 Washington Road, Princeton, New Jersey, NJ 08544, USA

8 ² Division of Virology, Pathogenesis and Cancer, Institute of Human Virology,
9 Departments of Pharmacology, Microbiology and Immunology, University of Maryland
10 School of Medicine, Baltimore, MD 21201, USA

11 ³ Lineberger Comprehensive Cancer Center, Department of Microbiology and
12 Immunology, The University of North Carolina at Chapel Hill, Chapel Hill, NC 27599,
13 USA

14 ⁴ Department of Pathology, New York University Medical Center, New York, NY 10016,
15 USA

16 ^ These authors contributed equally.

17 * Present address: Memorial Sloan-Kettering Cancer Center, 1275 York Avenue, New
18 York, NY 10065, USA

19 ** Present address: Department of Microbiology, Boston University School of Medicine,
20 Boston, MA, USA. National Emerging Infectious Diseases Laboratories, Boston
21 University, Boston, MA, USA.

22 *** Present address: Department of Gastroenterology, Kanazawa University Graduate
23 School of Medicine, Kanazawa, Ishikawa, Japan

24 # Correspondence should be addressed to A.P. (aploss@princeton.edu) or L.S.
25 (lsu@ihv.umaryland.edu)

26 **Running head:** Advanced humanized mouse models of HBV and HIV coinfection
27 **Keywords:** Hepatitis B virus; HBV; HIV, AIDS, antiviral immunity; humanized mice;
28 species tropism

29 **ABSTRACT**

30 Chronic hepatitis B (CHB), caused by hepatitis B virus (HBV), remains a major medical
31 problem. HBV has a high propensity for progressing to chronicity and can result in
32 severe liver disease, including fibrosis, cirrhosis and hepatocellular carcinoma. CHB
33 patients frequently present with viral coinfection, including HIV and hepatitis delta virus.
34 About 10% of chronic HIV carriers are also persistently infected with HBV which can
35 result in more exacerbated liver disease. Mechanistic studies of HBV-induced immune
36 responses and pathogenesis, which could be significantly influenced by HIV infection,
37 have been hampered by the scarcity of immunocompetent animal models. Here, we
38 demonstrate that humanized mice dually engrafted with components of a human
39 immune system and a human liver supported HBV infection, which was partially
40 controlled by human immune cells, as evidenced by lower levels of serum viremia and
41 HBV replication intermediates in the liver. HBV infection resulted in priming and
42 expansion of human HLA-restricted CD8+ T cells, which acquired an activated
43 phenotype. Notably, our dually humanized mice support persistent coinfections with HBV
44 and HIV which opens opportunities for analyzing immune dysregulation during HBV and
45 HIV coinfection and preclinical testing of novel immunotherapeutics.

46 INTRODUCTION

47 Hepatitis B virus (HBV) imposes a considerable disease burden globally. Approximately
48 257 million people are infected chronically with HBV (CHB), and are resultantly at
49 greater risk of developing cirrhotic liver disease and hepatocellular carcinoma ¹. About
50 one million deaths occur annually from CHB and, compared with 2016, projections for
51 2040 estimate that deaths due to liver cancer caused by HBV will almost double ².
52 Although de novo HBV infection can be effectively prevented via vaccination, and
53 viremia stably suppressed with direct-acting antivirals (DAAs), chronic HBV is largely
54 incurable ³. HBV infection often presents clinically in patients who have complex
55 conditions and coinfections with other viruses. One such virus is the human
56 immunodeficiency virus type 1 (HIV-1), for which there is neither a cure nor vaccine ⁴. Of
57 the 38 million people worldwide, who are infected with HIV, approximately 10% of them
58 are coinfecte with HBV ⁵.

59 It is noted that HIV infection can induce immunosuppression and inflammation that may
60 exacerbate HBV-mediated liver disease progression. However, most reports originated
61 from studies conducted before the highly active combination anti-retroviral therapy
62 (cART) entered widespread clinical use ⁶. Reverse transcriptase inhibitors can inhibit
63 replication of both HIV and HBV. This has affected the way in which these viruses
64 interface in patients receiving such treatment, and clinical studies of HBV and HIV
65 coinfection reveal the interpretational difficulties that can arise in this setting. For
66 example, one case study observed that lamivudine-inclusive cART had a propensity to
67 control occult HBV infection (OBI), given that discontinuation of it resulted in OBI
68 reactivation in a coinfecte patient ⁷. Prescription of cART has been used to explain the
69 observation that HBV coinfection in HIV-infected patients did not correlate with an
70 increased risk of hepatotoxicity ⁸. Conversely, coinfecte patients initiated on cART can
71 experience immune reconstitution inflammatory syndrome that differs from that
72 experienced by HBV-monoinfected patients ⁹. Some components of cART are also
73 hepatotoxic ¹⁰, which further complicates the treatment of patients coinfecte with HBV
74 and HIV.

75 Due to a scarcity of suitable, small animal models that recapitulate human-like features
76 of infection with these viruses, studies that explore the mechanisms that govern the

77 pathophysiology of HBV and HIV coinfection have been confined almost exclusively to
78 the clinic. This has resulted in a highly limited, and sometimes contradictory,
79 understanding of how these viruses interact with each other and their host. For example,
80 it has been noted that the immune reconstitution in response to HIV suppression by
81 cART could enhance the rate at which seroconversion of HBV antigens occurs ¹¹. It has
82 been postulated that a cART-induced rise in CD4+ T cells could accelerate the immune
83 response to HBV in coinfecting patients ¹², presumably by enhancing antigen
84 presentation and thereby antibody production against HBV. Other reports question the
85 validity of using CD4+ T-cell count as an indicator of treatment efficacy, given the
86 evidence that patients can fail to stabilize inflammation despite significant rises in CD4+
87 T-cells ¹³.

88 Until an animal model is made that recapitulates faithfully and authentically (some
89 aspects of) HIV-exacerbated viral hepatitis, elucidating the mechanisms underlying the
90 common and serious diseases caused by these pathogens and the development of
91 effective therapies will be impeded. Humanized mice, i.e. animals engrafted with human
92 tissues and/or expressing human genes, have emerged as a versatile experimental
93 model to study human-tropic viruses. As HBV requires a humanized liver for its life cycle,
94 robust engraftment of human hepatocytes has been established in a number of
95 immunodeficient liver injury models, including Alb-uPA ¹⁴, FAH^{-/-} ¹⁵, MUP-uPA ¹⁶, and
96 HSV-TK ¹⁷ mice. The resultant human liver chimeric mice support HBV infection and
97 have been used to study innate host responses to HBV and for testing the efficacy of
98 novel therapeutic regimens. However, the highly immunocompromised status of these
99 human liver chimeric mice precludes the study of immune-mediated pathogenesis by
100 HBV.

101 To enable analysis of human immune responses to HBV and HIV, protocols are being
102 designed to co-engage mice with human hepatocytes and components of a human
103 immune system (HIS). Double humanization of both the liver and immune system has
104 been achieved with human hematopoietic stem cells (HSCs) and either adult ^{18,19} or fetal
105 ²⁰ hepatocytes. Maturation of fetal hepatoblasts by exogenous administration of human
106 oncostatin M considerably boosted human hepatic chimerism, affirming that less mature
107 hepatic cells do not proliferate in response to liver injury in these xenorecipients. Dually

108 engrafted mice can support HBV infection, and studies have shown that viral infection
109 triggers activation of the engrafted HIS ¹⁹, in particular natural killer (NK) cells ²⁰ and M2
110 macrophages ²¹, and leads to some virally induced histopathology ²¹. A dually
111 humanized HSV-TK mouse model has also been created for the study of liver disease
112 induced by HIV ²². However, to date, a humanized mouse model has yet to be realized
113 that can support HBV and HIV coinfection, and that maps on closely to the viral kinetics
114 observed in patients.

115 As the impact of HIV coinfection on patients with CHB is ill-defined, developing a small
116 animal model to investigate this is an urgent need. This can be accomplished by tracking
117 HBV-specific adaptive immunity in the context of HIV coinfection. Priming and
118 maintenance of HBV antigen-specific T-cell responses have not been clearly understood
119 during HBV infection, which is a major impediment, considering that T cells play a critical
120 role in immune control of HBV. Here, we demonstrate that mice co-engrafted with
121 human liver tissue and a humanized immune system are susceptible to persistent HBV
122 and HIV coinfection, and mount HBV-specific immune responses which can be tracked
123 with MHC-tetramers. This new animal model holds promise for gaining mechanistic
124 insights into virus-mediated immune dysfunction and immunopathogenesis mediated by
125 HBV and HIV coinfection.

126 **RESULTS**

127 **FNRG/A2 mice support robust dual engraftment of human hepatic and**
128 **hematopoietic cells**

129 Development of functional adaptive immune responses is limited in HIS mice by the lack
130 of human leukocyte antigen (HLA) gene expression in mouse thymic epithelial cells.
131 Transgenic expression of a common human MHC class I allele, HLA-A2, has been
132 shown to significantly increase HLA-restricted human antiviral T-cell responses in Hu-
133 HIS mice infected with the human (lympho-)tropic pathogens Epstein-Barr virus (EBV),
134 HIV ²³, dengue virus ²⁴⁻²⁶ or yellow fever virus ²⁷. Thus, a transgenic FNRG mouse
135 expressing the HLA-A*0201 allele, hereafter referred to as FNRG/A2 mice, was
136 constructed to track HBV-specific CD8+ T cells (**Figure 1A**). To facilitate hepatic
137 engraftment, adult FNRG/A2 mice were intrasplenically injected with adult primary
138 human hepatocytes (PHH). Between 10-14 days thereafter, PHH-injected and non-
139 injected FNRG/A2 mice were subjected to sublethal irradiation and injected
140 intravenously with HLA-matched human hematopoietic stem cells (HSCs). Human
141 hematopoietic chimerism was similar in singly and dually repopulated mice, reaching ca.
142 20-25% of total CD45+ leukocytes in peripheral blood by 10 weeks post HSC injection
143 (**Figure 1B**). The human peripheral blood mononuclear cell (PBMC) fraction contained
144 CD3+ (both CD4+ and CD8+) T cells, B cells and, to a lesser extent, NK and myeloid
145 cells (**Supplementary Figure 1**), which is largely in line with previous reports. The
146 frequencies of the major human leukocyte subsets – including B, CD4+ and CD8+ T
147 cells, NK cells and various myeloid populations – in the peripheral blood, spleen and
148 liver were similar overall (**Supplementary Figure 1**). Consistent with our previous
149 results in FNRG mice ²⁸, FNRG/A2 supported robust engraftment with PHHs as
150 indicated by human albumin concentrations reaching >5 mg/ml (**Figure 1D**) and
151 detection of human FAH+ cells in the liver parenchyma (**Figure 1E**), yielding an
152 estimated human hepatic chimerism of 50-80%. Of note, there was no statistically
153 significant difference in the human hematopoietic engraftment between singly and dually
154 engrafted cohorts of mice. Collectively, these data are in line with reports detailing dual
155 humanization of the hepatic and hematopoietic compartments using allogenic cell
156 sources ^{18,29}. Notably, long-term dual reconstitution, without any evidence of hepatocyte
157 rejection by the HIS, was sustained even when the human cells were mismatched in

158 their major histocompatibility complex^{18,29}. This latter observation is consistent with the
159 limited HLA matching in human liver transplants, presumably due to the tolerogenic
160 microenvironment of the liver. This may also be due to pre-engraftment of PHHs to
161 induce tolerance during human HSC differentiation in the dually engrafted mice.

162

163 **Human immune cells partially control HBV infection in dually humanized mice**

164 Next, HBV infection kinetics were characterized in hepatocyte-only (HEP), HIS-only and
165 dually engrafted (HIS-HEP) mice. Consistent with previous reports^{14,15,28,30}, HBV viremia
166 was readily detectable in the serum of HEP and HIS-HEP mice within 2 weeks of
167 intravenous inoculation and plateaued at ca. 4 weeks (**Figure 2A, B**). In dually engrafted
168 mice, HBV DNA (**Figure 2A**) and HBV surface antigen (HBsAg) (**Figure 2B**) reached
169 similar levels by 2 weeks post infection (wpi), but viremia subsequently decreased
170 relative to HEP-only mice, suggesting some level of control by the engrafted HIS. These
171 data were further corroborated by significantly lower copy numbers of intrahepatic HBV
172 DNA (**Figure 2C**) and pregenomic RNA (pgRNA) (**Figure 2D**) 6 wpi in HIS-HEP versus
173 HEP mice. Notably, levels of covalently closed circular DNA (cccDNA), a crucial marker
174 for HBV persistence (**Figure 2E**), were similar between the cohorts. In line with these
175 observations, HBV core antigen (HBcAg)-expressing cells were readily detectable in the
176 livers of HEP mice (**Figure 2F**) unlike in the HIS-HEP mice (**Figure 2G**). Expectedly,
177 singly engrafted HIS control mice, which do not harbor HBV-permissive, human
178 hepatocytes, remained aviremic (**Figure 2C-E**). Collectively, these data demonstrate
179 that, in this model, an engrafted HIS can partially control HBV infection but did not clear
180 the infection or reduce HBV cccDNA within the 6-week study period.

181

182 **HLA-restricted CD8+ T cells acquire an activated phenotype during HBV infection**

183 To determine whether the engrafted HIS in HIS-HEP mice would respond to HBV
184 infection and prime HBV antigen-specific T cells, cohorts of HIS and HIS-HEP mice
185 engrafted with A2+ HSCs and A2+ PHHs were infected with HBV, and human
186 leukocytes subjected to flow cytometric analysis. Overall, the frequencies of the major
187 lymphoid and myeloid subsets – including B, CD4+ and CD8+ T cells, NK cells and
188 various myeloid populations – in the peripheral blood, spleen and liver did not change
189 significantly upon infection (**Supplementary Figure 1**). To detect and quantify the

190 frequencies of HBV-specific T cells, an HLA-A*0201-restricted HBcAg-derived epitope
191 (FLPSDFFPSV) tetramer was used, which can assess virus-specific T-cell immunity in
192 HBV-infected patients³¹. In response to HBV infection, dually engrafted HIS-HEP but not
193 HIS mice, mounted human HLA-A*0201-restricted HBcAg-specific (FLPSDFFPSV)
194 CD8+ T-cell responses in the spleen and livers (**Figure 3A, B**). The cell-surface
195 phenotype of the antigen-specific cells, and thus co-stained FLPSDFFPSV:HLA-
196 A2*0201-tetramer+ CD8+ T cells, was determined by staining for several activation and
197 exhaustion markers, including PD1, CCR7, CD38, HLA-DR, CD45RA and CD127. Akin
198 to data in patients, some spread in the overall levels of surface expression was observed
199 (**Figure 3C, D**). In the liver of HIS-HEP mice, the activation markers HLA-DR1 and
200 CD127 were significantly upregulated on tetramer+ CD8+ T cells (**Figure 3C, D**). In the
201 spleen, only CD127 expression reached statistical significance (**Figure 3E**).

202 Collectively, these data provide evidence that HBV-specific T cells are primed during
203 viral infection in humanized mice. Notably, previously developed dual chimeric HIS-HEP
204 mice have only been generated using conventional immunodeficient liver injury mice and
205 therefore were unable to develop antigen-specific responses^{18,21,29}. Thus, this novel
206 model opens opportunities to mechanistically dissect HBV-induced immune dysfunction
207³². In NSG/A2-hu HSC mice treated with anti-mouse Fas mAb, similar findings were
208 reported with A2/HBc-specific CD8+ T cells. Interestingly, those tetramer+ CD8 T cells
209 were reduced in their ability to respond to HBcAg *in vitro* relative to similar CD8+ T cells
210 from the spleen²¹. It will be of interest to study the functional difference between HBV-
211 specific T cells in the spleen and in the liver.

212
213 **Limited evidence of immune-mediated liver injury during an acute HBV infection in**
214 **HIS-HEP mice**

215 Although the mechanisms underlying liver disease in HBV-infected patients are not fully
216 understood, it is thought that the inflammatory milieu in the liver during infection is a
217 significant driver of hepatic pathology. Thus, we sought to determine whether we could
218 observe any evidence of HBV-induced liver injury in our model. There were no
219 discernable differences in the overall appearance of the liver tissue and no evidence of
220 fibrosis in either infected or non-infected HIS, HEP, or HIS-HEP mice during the acute

221 phase of HBV infection (**Figure 4A-F**). Overt liver disease is rare in HBV-infected
222 patients during the acute phase of the infection. The apparent lack of liver disease in our
223 model is also largely in agreement with previous observations in dually humanized mice
224^{19,20} and may be attributed to the overall impaired function of the engrafted immune
225 system and/or the lack of human non-parenchymal cells in the liver which may aid in
226 driving disease progression. Furthermore, liver disease is far more exacerbated in
227 patients chronically infected with HBV for many months to years and thus the time
228 course will likely have to be extended beyond the current 6-week study period to
229 observe a liver injury phenotype. In NSG/A2-hu HSC mice co-transplanted with fetal
230 hepatoblasts, and treated with anti-mouse Fas mAb, low HBV replication is detected and
231 persistent HBV infection for 14-16 wpi leads to liver diseases associated with induction
232 of human M2-like macrophages²¹. It will be of interest to investigate HBV-induced liver
233 diseases in the HIS-HEP model during chronic, persistent infection and with additional
234 cofactors.

235

236 **Dually humanized mice can support persistent coinfection with HBV and HIV-1**

237 We aimed to determine whether dually engrafted mice would support HBV and HIV
238 coinfection. It has previously been demonstrated that deletion of the murine *Flk2* gene
239 (*Flk2*^{-/-}) severely impairs the development of various myeloid cell types, including
240 dendritic cells (DC)³³. It has also been shown by our group that exogenous
241 administration of human Flt3LG promotes the expansion of human DCs and NK cells,
242 while leaving such cells of murine origin unaffected in *Flk2*^{-/-} humanized mice²⁷. Thus,
243 FNRG/A2-hu HIS-HEP mice deficient in *Flk2* (FNRG/A2-hu HIS-HEP) were generated.
244 Cohorts of dually humanized FNRG/A2-hu HIS-HEP mice were first infected
245 intraperitoneally with HBV and subsequently with HIV. Mice were then treated with
246 Flt3LG to promote myeloid and NK cell expansion (**Figure 5A**). These dually humanized
247 mice supported persistent HBV and HIV coinfection, as evidenced by serum HBsAg
248 (**Figure 5B**), HBV DNA and pgRNA in the liver (**Figure 5C**), and serum HIV RNA
249 (**Figure 5D**). Over the six-week study period, no overt effect of HIV on HBV infection
250 metrics was observed, and vice versa. However, differences may become more
251 apparent over longer periods of coinfection, and inclusion of additional parameters (i.e.

252 functionality of T cells, number of HIV+ cells, mutation rate in either virus, etc.).
253 Collectively, this FNRGF/A2-hu HIS-HEP mouse model is well suited for such studies.

254

255 **Dually humanized mice experience coinfection-dependent differences in viral titer**
256 **and humanized immunity**

257 Finally, we aimed to determine if our model can recapitulate fundamental features of
258 HBV and HIV coinfection that are observed clinically. To do this, we examined our
259 FNRGF/A2-hu HIS-HEP model under various settings of infection, including uninfected
260 mice and those singly and coinfecte with HBV and/or HIV. Mice to be coinfecte were
261 infected first with HBV, followed by HIV, and all mice were bled several times over 15
262 weeks, followed by liver harvest (**Figure 6A**). The presence of HBV DNA in the blood of
263 coinfecte mice and those singly infected with HBV (**Figure 6B**), and the presence HIV
264 RNA in coinfecte mice and those singly infected with HIV (**Figure 6C**) was then
265 confirmed. HIV and HBV did not significantly affect each other's replication, as
266 determined by viremias in the blood.

267 We next quantified changes in gene expression in terms of HBV pgRNA (**Figure 6D**)
268 and HIV RNA (**Figure 6E**) in the livers of these animals. While no significant difference
269 was calculated in terms of HBV pgRNA expression in the livers of HBV-monoinfected
270 mice compared with coinfecte mice, changes in expression ranging from hundred-fold
271 to thousand-fold were frequently recorded in the liver of coinfecte animals. This
272 substantiates what is known clinically about the exacerbation of HBV-related disease in
273 coinfecte patients not receiving cART. Similarly, no significant difference was detected
274 in terms of HIV RNA expression in the livers of HIV-monoinfected mice compared with
275 coinfecte mice; however, a trend in increased HIV gene expression/replication in
276 coinfecte mice was also noted.

277 HBV/HIV coinfections are known to result in more severe liver disease than HBV mono-
278 infections, and thus we aimed to gather evidence of whether such a phenotype could
279 possibly be recapitulated in our dually humanized mice. We thus quantified the
280 expression of various human genes, related to inflammation and liver disease, by RT-
281 qPCR in the livers of these animals (**Figure 7**). This analysis included human
282 macrophage markers and fibrosis genes – CD163, arginase 1 (ARG1), tissue inhibitor of

283 metalloproteinase-1 (TIMP-1), and transforming growth factor beta (TGF- β 1), in addition
284 to several interferon (IFN)-stimulated genes (ISGs), including interferon-induced
285 transmembrane protein 3 (IFITM3), ISG15, IFN- β , myxovirus resistance protein 1 (Mx1),
286 2'-5'-oligoadenylate synthetase 1 (OAS1), and the cytidine deaminase APOBEC3G
287 (APO3G). These markers are commonly analyzed in the contexts of HIV infection and
288 coinfection with HBV^{34,35}. HBV is considered a stealth virus that does not result in
289 significant dysregulation of host inflammation in the liver³⁶, which is also corroborated
290 by our preliminary data (**Figure 7**). Remarkably, there was a trend towards more
291 pronounced expression of all 10 genes in HBV/HIV coinfecting mice, as compared with
292 the naïve and singly infected mice, but only hOAS1 expression reached statistical
293 significance between the HBV and HBV/HIV coinfection groups (**Figure 7C**).
294 Collectively, our data suggest that HBV/HIV co-infection results in dysregulation of
295 numerous host genes in the liver of our dually humanized mice that mirrors what is
296 observed in coinfecting patients.

297 **DISCUSSION**

298 The complex interplay between HBV, HIV, and the human host remains opaque in part
299 due to the limited availability of immunocompetent animal models. Some basic and
300 central questions are controversial, such as whether HBV can influence HIV
301 pathogenesis at all. Some studies note that HIV is apparently unaffected by HBV
302 coinfection ³⁷, while others have observed that patients positive for HBeAg experience
303 slower responses to cART ³⁸. Furthermore, *in vitro* studies have shown that the X-protein
304 of HBV can super-induce HIV-1 replication ³⁹, which corroborates what is observed in
305 our model. The lack of fundamental understanding of the true nature of HBV/HIV
306 coinfection calls urgently for a reproducible, robust model that can accurately map onto
307 the clinical reality. The dually engrafted models described here hold promise for
308 addressing elusive and fundamental questions in HBV and HIV coinfection virology and
309 pathogenesis.

310 One of the ways in which the impact of HIV on HBV infection might be assessed is by
311 tracking T cells specific for HBV antigens. Immune tolerance and development of a
312 chronic HBV infection are thought to result, at least in part, from a dysfunctional CD8+ T-
313 cell response ⁴⁰. In chimpanzees experimentally infected with HBV, it was shown that an
314 HBV-specific CD8+ T-cell response was key to viral clearance ⁴¹. It has also been
315 observed that CD8+ T cells from chronically infected patients are more prone to having
316 an exhausted phenotype as indicated by high levels of programmed death 1 (PD1)
317 molecule, while levels of PD1 are low in acutely infected patients ⁴². In other reports,
318 CD8+ T cells in chronically infected patients have been shown to express higher levels
319 of TIM3 and cytotoxic T-lymphocyte antigen-4 (CTLA-4) than those of acutely infected or
320 naïve patients, also indicating an exhausted phenotype ⁴³. In addition, a lower frequency
321 of HBV-specific tetramer-stained CD8+ T cells have been isolated from chronic as
322 opposed to acutely infected patients ⁴². Notably, *ex vivo* CD8+ T cells from chronically
323 infected patients or HBV transgenic mice exhibit a less activated phenotype and are
324 impaired in the ability to produce effector cytokines ^{42,44}. The critical importance of the
325 CD8+ T-cell response has been further confirmed as CD8+ T cells, engineered to
326 recognize HBV antigens when adoptively transferred into human liver chimeric
327 uPA/SCID mice, resulted in reduced viremia in both the serum and liver, indicating the
328 ability of these engineered CD8+ T cells to control HBV infection ⁴⁵. As an HBV-specific

329 CD8+ T-cell response in HBV infected dually engrafted FNRG/A2 animals was observed
330 in the present work, further characterization of this phenotype and the kinetics of this
331 response in our HBV/HIV coinfection animal model could shed light on the parameters
332 affecting CD8+ T cell functions in coinfecting patients.

333 Undoubtedly, humanized mice cannot (yet) perfectly mimic the complex situation of
334 chronic HBV and HIV coinfection in patients, but important aspects of it can be
335 recapitulated, as shown here. Future refinements will focus on improving the limited
336 functionality of the engrafted HIS. Numerous strategies to do this have been proposed
337 (reviewed in ⁴⁶) as several human cell lineages remain underrepresented in part due to
338 the orthologs of non-redundant cytokines, which exhibit limited biological cross-reactivity.
339 Our lab has previously shown that selective expansion of under-represented cell types,
340 such as dendritic cells, NK cells and granulocytes, leads to markedly improved immune
341 responses to the yellow fever virus (YFV) vaccine akin to those observed in YFV
342 vaccines ²⁷. Additionally, the development of functional adaptive immune responses is
343 limited by the lack of HLA gene expression. Expressing a human MHC class I allele has
344 multiple benefits as it allows for more faithful development of CD8+ T cells in the thymus,
345 enables recognition of (viral) antigens in peripheral tissues by human CD8+ T cells and
346 facilitates tracking of antigen-specific CD8+ T cells with MHC multimers, as previously
347 shown for EBV, dengue virus ²⁴⁻²⁶ and, here in our study for the first time, HBV.

348 A shortcoming of our animal models is the lack of human MHC class II expression,
349 which may result in CD4+ T-cell lineage dysfunctions. It has previously been suggested
350 that expression of a human MHC class II molecule, HLA-DR4, partially improves the
351 development of functional human T and B cells ⁴⁷. Our lab previously characterized
352 adaptive immune responses to adenovirus infections in humanized HLA-A*0201 and
353 HLA-DRB*01 doubly transgenic mice, finding statistically significant clearance of viral
354 antigens from the liver ⁴⁸. Thus, combining the FNRG/A2 mice with a human MHC II
355 transgenic model may be an immediate improvement. This would be particularly
356 important when investigating the impact of HIV on CD4+ T cell exhaustion, and their
357 function in helping B cells to induce HBsAg antibodies during HBV functional cure. As
358 such, the immune response in HBV/HIV-challenged, dually engrafted, human MHC class
359 II-expressing FNRG/A2 mice could more faithfully recapitulate the response observed

360 in human patients. Co-engraftment of improved xenorecipient strains with additional
361 HSC donor-matched human tissues, such as liver, thymus and/or lymph nodes, could
362 also significantly augment the immune response. Such co-engraftments could enhance
363 T- and B-cell selection, intra-hepatic T-cell priming ⁴⁹ and liver-mediated secretion of key
364 human-immune components ⁵⁰. Finally, engraftment of second-generation humanized
365 mice with a human-like microbiome represents another valuable approach to enhance
366 immunity, as recently suggested ⁵¹.

367 While the above-mentioned modifications will undoubtedly aid in improving our
368 FNRGF/A2 dually humanized mouse model, the current FNRGF/A2-hu HIS-HEP mouse
369 has already considerable utility. Here, we show that these dually engrafted animals can
370 elicit an HBV-specific T-cell response phenotypically similar to what is observed in
371 acutely infected HBV patients, and can sustain long-term, clinically relevant HBV and
372 HIV coinfection. We have demonstrated that our humanized mouse model can be used
373 effectively to interrogate transcriptional changes that occur between mono-infection and
374 coinfection with HBV and HIV, that could influence hepatic disease progression in
375 patients coinfected with these viruses. By cross-examining changes in liver histology
376 with dysregulated expression of these genes, for example, we can gain keen insights
377 into how HBV and HIV cooperate to elicit different mechanisms of disease than when
378 they singly infect patients. Although we did not see any significant signs of liver damage
379 or disease, this is most likely because the current study was limited to a relatively short
380 period of time whereas it takes months to years for chronic HBV infection to result in liver
381 disease in humans. Of note, previous work in a different type of dually engrafted mice
382 observed that inflammatory M2 macrophages were more abundant in mice dually
383 engrafted with human hepatocytes and a HIS as compared with non-infected dually
384 engrafted mice ²¹. Future studies in our model or further refined versions will probe
385 whether HBV/HIV coinfection results in accelerated liver disease mediated by the
386 aforementioned M2-like macrophages or other lymphoid cell populations.

387 **MATERIALS AND METHODS**

388 A detailed description of the Materials and Methods used in this study is included in the
389 supplementary information.

390

391 **Authors' contributions**

392 G.H., B.Y.W., J.A., L.S., and A.P. designed and performed experiments and wrote the
393 manuscript. T.S.H., F.D., M.F., and J.S. performed experiments and analysis. L.C.
394 performed experiments.

395

396 **Competing financial interests.** The authors declare no relevant conflicts of interest.

397

398 **Acknowledgments**

399 HepG2.2.15 cells were kindly provided by Christoph Seeger (Fox Chase Cancer Center,
400 FCCC). We thank Gabriela Hrebikova for technical assistance and Christina DeCoste
401 and the Molecular Biology Flow Cytometry Resource Facility, which is partially supported
402 by the Cancer Institute of New Jersey Cancer Center Support Grant (P30CA072720. We
403 are grateful to Jenna Gaska, Florian Douam, and members of the Ploss lab for critical
404 discussions and edits of this manuscript. This study was supported by grants from the
405 National Institutes of Health (R01 AI138797 to A.P. and L.S., R01 AI153236, R01
406 AI146917, R01 AI168048 all to A.P), a Research Scholar Award from the American
407 Cancer Society (RSG-15-048-01-MPC to A.P.), a Burroughs Wellcome Fund Award for
408 Investigators in Pathogenesis (to A.P.) a Graduate fellowship from the Health Grand
409 Challenge from the Global Health Fund of Princeton University (to B.Y.W.). The NYU
410 Experimental Pathology Immunohistochemistry Core Laboratory is supported in part by
411 the Laura and Isaac Perlmutter Cancer Center Support Grant; NIH /NCI P30CA016087”
412 and the National Institutes of Health S10 Grants; NIH/ORIP S10OD01058 and
413 S10OD018338. B.Y.W. was a recipient of F31 NIH/NRSA Ruth L. Kirschstein
414 Predoctoral awarded from the NIAID and a graduate fellowship from the New Jersey
415 Commission on Cancer Research and was supported by an NIH training grant
416 (T32GM007388). J.S. was a recipient of a postdoctoral fellowships from the German
417 Research Foundation.

418

419 REFERENCES

420 1. Asselah T, Loureiro D, Boyer N, Mansouri A. Targets and future direct-acting
421 antiviral approaches to achieve hepatitis B virus cure. *Lancet Gastroenterol
422 Hepatol.* 2019;4(11):883-892.

423 2. Foreman KJ, Marquez N, Dolgert A, et al. Forecasting life expectancy, years of
424 life lost, and all-cause and cause-specific mortality for 250 causes of death:
425 reference and alternative scenarios for 2016-40 for 195 countries and territories.
426 *Lancet.* 2018;392(10159):2052-2090.

427 3. Martinez MG, Villeret F, Testoni B, Zoulim F. Can we cure hepatitis B virus with
428 novel direct-acting antivirals? *Liver Int.* 2020;40 Suppl 1:27-34.

429 4. Davenport MP, Khouri DS, Cromer D, Lewin SR, Kelleher AD, Kent SJ.
430 Functional cure of HIV: the scale of the challenge. *Nat Rev Immunol.*
431 2019;19(1):45-54.

432 5. Platt L, French CE, McGowan CR, et al. Prevalence and burden of HBV co-
433 infection among people living with HIV: A global systematic review and meta-
434 analysis. *J Viral Hepat.* 2020;27(3):294-315.

435 6. Kim HN. Chronic Hepatitis B and HIV Coinfection: A Continuing Challenge in the
436 Era of Antiretroviral Therapy. *Curr Hepatol Rep.* 2020;19(4):345-353.

437 7. Costantini A, Marinelli K, Biagioni G, et al. Molecular analysis of hepatitis B virus
438 (HBV) in an HIV co-infected patient with reactivation of occult HBV infection
439 following discontinuation of lamivudine-including antiretroviral therapy. *BMC
440 Infect Dis.* 2011;11:310.

441 8. Núñez M, Lana R, Mendoza JL, Martín-Carbonero L, Soriano V. Risk factors for
442 severe hepatic injury after introduction of highly active antiretroviral therapy. *J
443 Acquir Immune Defic Syndr.* 2001;27(5):426-431.

444 9. Mitsumoto F, Murata M, Kato Y, et al. Hepatitis B virus-related immune
445 reconstitution inflammatory syndrome in two patients coinfecting with human
446 immunodeficiency virus diagnosed with a liver biopsy. *Intern Med.*
447 2014;53(18):2165-2170.

448 10. Sulkowski MS. Viral hepatitis and HIV coinfection. *J Hepatol.* 2008;48(2):353-
449 367.

450 11. Mialhes P, Trabaud MA, Pradat P, et al. Impact of highly active antiretroviral
451 therapy (HAART) on the natural history of hepatitis B virus (HBV) and HIV
452 coinfection: relationship between prolonged efficacy of HAART and HBV surface
453 and early antigen seroconversion. *Clin Infect Dis.* 2007;45(5):624-632.

454 12. Jiang T, Su B, Song T, et al. Immunological Efficacy of Tenofovir Disoproxil
455 Fumarate-Containing Regimens in Patients With HIV-HBV Coinfection: A
456 Systematic Review and Meta-Analysis. *Front Pharmacol.* 2019;10:1023.

457 13. Tincati C, Mondatore D, Bai F, d'Arminio Monforte A, Marchetti G. Do
458 Combination Antiretroviral Therapy Regimens for HIV Infection Feature Diverse
459 T-Cell Phenotypes and Inflammatory Profiles? *Open Forum Infect Dis.*
460 2020;7(9):ofaa340.

461 14. Meuleman P, Libbrecht L, De Vos R, et al. Morphological and biochemical
462 characterization of a human liver in a uPA-SCID mouse chimera. *Hepatology.*
463 2005;41(4):847-856.

464 15. Bissig KD, Wieland SF, Tran P, et al. Human liver chimeric mice provide a model
465 for hepatitis B and C virus infection and treatment. *J Clin Invest.*
466 2010;120(3):924-930.

467 16. Tesfaye A, Stift J, Maric D, Cui Q, Dienes HP, Feinstone SM. Chimeric mouse
468 model for the infection of hepatitis B and C viruses. *PLoS One.*
469 2013;8(10):e77298.

470 17. Kosaka K, Hiraga N, Imamura M, et al. A novel TK-NOG based humanized
471 mouse model for the study of HBV and HCV infections. *Biochem Biophys Res
472 Commun.* 2013;441(1):230-235.

473 18. Gutti TL, Knibbe JS, Makarov E, et al. Human hepatocytes and hematolymphoid
474 dual reconstitution in treosulfan-conditioned uPA-NOG mice. *The American
475 journal of pathology.* 2014;184(1):101-109.

476 19. Dusseaux M, Masse-Ranson G, Darche S, et al. Viral Load Affects the Immune
477 Response to HBV in Mice With Humanized Immune System and Liver.
478 *Gastroenterology.* 2017;153(6):1647-1661 e1649.

479 20. Billerbeck E, Mommersteeg MC, Shlomai A, et al. Humanized mice efficiently
480 engrafted with fetal hepatoblasts and syngeneic immune cells develop human
481 monocytes and NK cells. *J Hepatol.* 2016;65(2):334-343.

482 21. Bility MT, Cheng L, Zhang Z, et al. Hepatitis B virus infection and
483 immunopathogenesis in a humanized mouse model: induction of human-specific
484 liver fibrosis and M2-like macrophages. *PLoS Pathog.* 2014;10(3):e1004032.

485 22. Dagur RS, Wang W, Makarov E, Sun Y, Poluektova LY. Establishment of the
486 Dual Humanized TK-NOG Mouse Model for HIV-associated Liver Pathogenesis.
487 *J Vis Exp.* 2019(151).

488 23. Cheng L, Ma J, Li G, Su L. Humanized Mice Engrafted With Human HSC Only or
489 HSC and Thymus Support Comparable HIV-1 Replication, Immunopathology,
490 and Responses to ART and Immune Therapy. *Front Immunol.* 2018;9:817.

491 24. Shultz LD, Saito Y, Najima Y, et al. Generation of functional human T-cell
492 subsets with HLA-restricted immune responses in HLA class I expressing
493 NOD/SCID/IL2r gamma(null) humanized mice. *Proc Natl Acad Sci U S A.*
494 2010;107(29):13022-13027.

495 25. Strowig T, Gurer C, Ploss A, et al. Priming of protective T cell responses against
496 virus-induced tumors in mice with human immune system components. *J Exp
497 Med.* 2009;206(6):1423-1434.

498 26. Jaiswal S, Pearson T, Friberg H, et al. Dengue virus infection and virus-specific
499 HLA-A2 restricted immune responses in humanized NOD-scid IL2rgamma null
500 mice. *PLoS One.* 2009;4(10):e7251.

501 27. Douam F, Ziegler CGK, Hrebikova G, et al. Selective expansion of myeloid and
502 NK cells in humanized mice yields human-like vaccine responses. *Nat Commun.*
503 2018;9(1):5031.

504 28. Winer BY, Huang T, Low BE, et al. Recapitulation of treatment response patterns
505 in a novel humanized mouse model for chronic hepatitis B virus infection.
506 *Virology.* 2017;502:63-72.

507 29. Wilson EM, Bial J, Tarlow B, et al. Extensive double humanization of both liver
508 and hematopoiesis in FRGN mice. *Stem Cell Res.* 2014;13(3 Pt A):404-412.

509 30. Dandri M, Burda MR, Tordok E, et al. Repopulation of mouse liver with human
510 hepatocytes and in vivo infection with hepatitis B virus. *Hepatology.*
511 2001;33(4):981-988.

512 31. Bengsch B, Martin B, Thimme R. Restoration of HBV-specific CD8+ T cell
513 function by PD-1 blockade in inactive carrier patients is linked to T cell
514 differentiation. *J Hepatol*. 2014;61(6):1212-1219.

515 32. Tran TT. Immune tolerant hepatitis B: a clinical dilemma. *Gastroenterol Hepatol*
516 (N Y). 2011;7(8):511-516.

517 33. Waskow C, Liu K, Darrasse-Jèze G, et al. The receptor tyrosine kinase Flt3 is
518 required for dendritic cell development in peripheral lymphoid tissues. *Nat
519 Immunol*. 2008;9(6):676-683.

520 34. Ahodantin J, Nio K, Funaki M, et al. Type I interferons and TGF- β cooperate to
521 induce liver fibrosis during HIV-1 infection under antiretroviral therapy. *JCI
522 Insight*. 2022;7(13).

523 35. Cheng L, Yu H, Li G, et al. Type I interferons suppress viral replication but
524 contribute to T cell depletion and dysfunction during chronic HIV-1 infection. *JCI
525 Insight*. 2017;2(12).

526 36. Winer BY, Gaska JM, Lipkowitz G, et al. Analysis of Host Responses to Hepatitis
527 B and Delta Viral Infections in a Micro-scalable Hepatic Co-culture System.
528 *Hepatology*. 2020;71(1):14-30.

529 37. Chun HM, Mesner O, Thio CL, et al. HIV outcomes in Hepatitis B virus coinfecting
530 individuals on HAART. *J Acquir Immune Defic Syndr*. 2014;66(2):197-205.

531 38. Idoko J, Meloni S, Muazu M, et al. Impact of hepatitis B virus infection on human
532 immunodeficiency virus response to antiretroviral therapy in Nigeria. *Clin Infect
533 Dis*. 2009;49(8):1268-1273.

534 39. Gómez-Gonzalo M, Carretero M, Rullas J, et al. The hepatitis B virus X protein
535 induces HIV-1 replication and transcription in synergy with T-cell activation
536 signals: functional roles of NF-kappaB/NF-AT and SP1-binding sites in the HIV-1
537 long terminal repeat promoter. *J Biol Chem*. 2001;276(38):35435-35443.

538 40. Ye B, Liu X, Li X, Kong H, Tian L, Chen Y. T-cell exhaustion in chronic hepatitis
539 B infection: current knowledge and clinical significance. *Cell Death Dis*.
540 2015;6:e1694.

541 41. Thimme R, Wieland S, Steiger C, et al. CD8(+) T cells mediate viral clearance
542 and disease pathogenesis during acute hepatitis B virus infection. *J Virol*.
543 2003;77(1):68-76.

544 42. Boni C, Fisicaro P, Valdatta C, et al. Characterization of hepatitis B virus (HBV)-
545 specific T-cell dysfunction in chronic HBV infection. *J Virol*. 2007;81(8):4215-
546 4225.

547 43. Schurich A, Khanna P, Lopes AR, et al. Role of the coinhibitory receptor
548 cytotoxic T lymphocyte antigen-4 on apoptosis-prone CD8 T cells in persistent
549 hepatitis B virus infection. *Hepatology*. 2011;53(5):1494-1503.

550 44. Wang Q, Pan W, Liu Y, et al. Hepatitis B Virus-Specific CD8+ T Cells Maintain
551 Functional Exhaustion after Antigen Reexposure in an Acute Activation Immune
552 Environment. *Front Immunol*. 2018;9:219.

553 45. Kah J, Koh S, Volz T, et al. Lymphocytes transiently expressing virus-specific T
554 cell receptors reduce hepatitis B virus infection. *J Clin Invest*. 2017;127(8):3177-
555 3188.

556 46. Walsh NC, Kenney LL, Jangalwe S, et al. Humanized Mouse Models of Clinical
557 Disease. *Annu Rev Pathol*. 2017;12:187-215.

558 47. Suzuki M, Takahashi T, Katano I, et al. Induction of human humoral immune
559 responses in a novel HLA-DR-expressing transgenic NOD/Shi-scid/gammacnull
560 mouse. *Int Immunol.* 2012;24(4):243-252.

561 48. Billerbeck E, Horwitz JA, Labitt RN, et al. Characterization of human antiviral
562 adaptive immune responses during hepatotropic virus infection in HLA-transgenic
563 human immune system mice. *J Immunol.* 2013;191(4):1753-1764.

564 49. Huang LR, Wohlleber D, Reisinger F, et al. Intrahepatic myeloid-cell aggregates
565 enable local proliferation of CD8(+) T cells and successful immunotherapy
566 against chronic viral liver infection. *Nature immunology.* 2013;14(6):574-583.

567 50. Sander LE, Sackett SD, Dierssen U, et al. Hepatic acute-phase proteins control
568 innate immune responses during infection by promoting myeloid-derived
569 suppressor cell function. *J Exp Med.* 2010;207(7):1453-1464.

570 51. Gulden E, Vudattu NK, Deng S, et al. Microbiota control immune regulation in
571 humanized mice. *JCI insight.* 2017;2(21).

572

573 **FIGURE LEGENDS**

574 **Figure 1. Robust human hematopoietic and hepatic co-engraftment in FNRG/A2**
575 **mice. (A).** Schematic of overall experimental approach. FNRG/A2 mice were either
576 dually engrafted with human HSCs and hepatocytes, or HSCs alone. **(B).** Frequency of
577 hCD45+ cells in HIS-HEP and HIS mice. **(C).** Frequency of CD3+ T cells, CD19+ B cells,
578 and CD56+ NK cells. HIS-HEP and Hep only mice were bled and human albumin in the
579 serum quantified by ELISA **(D).** Human albumin concentrations in the sera of HIS-HEP
580 vs. HEP mice. **(E).** FAH staining of HIS-HEP engrafted mice corroborates human
581 hepatocyte engraftment. N=10 per group of HIS-HEP and HIS mice.

582

583 **Figure 2. Partial control of an acute HBV infection in dually engrafted FNRG/A2-hu**
584 **HIS-HEP mice. (A/B).** HBV infection kinetics were measured in serum by HBV DNA **(A)**
585 or HBsAg **(B).** **(C-G).** In the liver, total HBV DNA **(C)**, HBV pgRNA **(D)**, or HBV cccDNA
586 **(E)** were quantified by qPCR. Immunohistochemical staining for HBcAg was performed
587 on FNRG/A2-hu HIS-HEP mice **(F)** and FNRG/A2-hu HIS mice **(G)**. N=7-10 animals per
588 group. Error bars represent means \pm SEM. Multiple group comparisons were analyzed
589 by one-way ANOVA with a Bonferroni's multiple comparisons test. *p<0.05, **p \leq 0.01,
590 ****p \leq 0.0001.

591

592 **Figure 3. Priming and expansion of intrahepatic HBcAg-specific CD8+ T cells in**
593 **HBV-infected FNRG/A2-hu HIS-HEP mice.** FNRG/A2-hu HIS-HEP and FNRG/A2-hu
594 HIS mice were challenged with HBV, and their lymphocytes were isolated from livers
595 and spleens. **(A).** Representative FACS plots of hCD8+, HBV tetramer-positive cells.
596 **(B).** Quantification of the number of hCD8+ T cells positive for HBV core
597 FLPSDFPPSV/A2 tetramer staining from FNRG/A2-hu HIS-HEP (red) and FNRG/A2-hu
598 HIS mice (gray). **(C).** Representative FACS plots of hCD8+ T cells that were dually
599 positive for their respective activation markers (PD1, CCR7, CD38, HLA-DR, or
600 CD45RA) and the HBV core tetramer. **(D/E).** Quantification of CD8+ T cells in the liver
601 **(D)** and spleen **(E)** that were dually positive for respective activation marker (CCR7,
602 CD38, CD45RA, HLA-DR, PD-1, CD27, CD127, and CD28) and the HBV tetramer. N=7-
603 10 animals per group. Error bars represent means \pm SEM. Multiple group comparisons

604 were analyzed by one-way ANOVA with a Bonferroni's multiple comparisons test. *p
605 <0.05, ***p ≤ 0.001.

606 **Figure 4. Minor liver injury is observed in HIS-HEP vs HEP mice.** HBV infected HIS-
607 HEP, HIS, and HEP mice were euthanized 6 weeks post challenge with HBV. Mouse
608 livers were perfused and embedded in paraffin and H&E stained to ascertain if liver
609 damage had occurred. HBV-infected HIS (A), HEP (C), and HIS-HEP (E) and non-
610 infected HIS (B), HEP (D), and HIS-HEP (F) mice showed little evidence of liver
611 damage.

612

613 **Figure 5. HBV/HIV-1 coinfection in FNRGF/A2-hu HIS-HEP mice. (A.)** Schematic
614 representation of the experimental procedure for characterizing HBV and HIV-1 infection
615 in NRGF/A2-hu HIS mice and FNRGF/A2-hu HIS-HEP mice. (B.) Longitudinal HBsAg in
616 the serum of NRGF/A2-hu HIS (red) and FNRGF/A2-hu HIS-HEP (blue) mice following
617 HBV and HIV coinfection. (C.) HBV DNA and pgRNA copies per mg liver tissue in
618 coinfected NRGF/A2-hu HIS (red) and FNRGF/A2-hu HIS-HEP (blue) at termination (48
619 days post-HIV-1 infection and 54 days post-HBV infection). (D.) HIV viral load in the
620 serum of coinfected NRGF/A2-hu HIS (red) and FNRGF/A2-hu HIS-HEP mice (black)
621 during the first 37/31 days post HBV/HIV-1 coinfection, respectively. **p<0.01,
622 ****p<0.0001.

623

624 **Figure 6. HBV and HIV infection and replication in FNRGF/A2-hu HIS-HEP mice
625 infected with HBV and/or HIV. (A.)** Schematic representation of the experimental
626 procedure for single infection with HBV or HIV, and coinfection. (B.) Quantification of
627 HBV genomic DNA in the plasma of singly infected, coinfecting, and uninfected mice.
628 (C.) Quantification of HIV genomic RNA in the plasma of singly infected, coinfecting, and
629 uninfected mice. (D.) Quantification of HBV pgRNA in the livers of singly infected,
630 coinfecting, and uninfected mice (relative to human GAPDH). (E.) Quantification of HIV
631 RNA in the livers of singly infected, coinfecting, and uninfected mice (relative to human
632 GAPDH). Error bars represent means ± SEM. Significance was determined via the
633 Kruskal-Wallis test. *p<0.05.

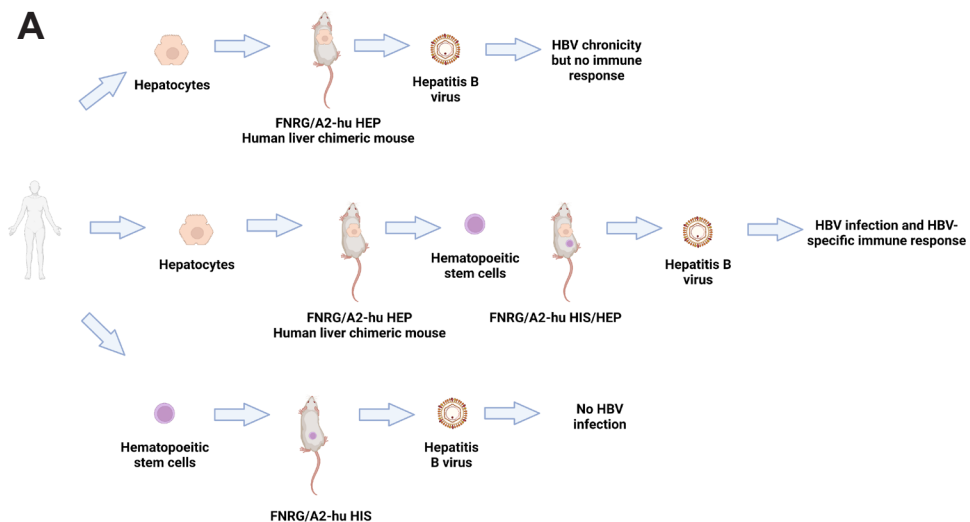
634

635 **Figure 7. Induction of human interferon-stimulated genes (ISG), and human M2
636 macrophage and fibrosis genes in the livers of FNRGF/A2-hu HIS-HEP mice singly
637 infected or coinfecte**d with HBV and/or HIV, and uninfected mice. (A-F). ISGs
638 investigated were (A) IFN- β , (B) IFITM3, (C) OAS1, (D) ISG-15, (E) Mx1, and (F)
639 APO3G. (G-J). Macrophage and fibrosis genes investigated were (G) CD163, (H) ARG1,
640 (I) TGF- β 1, and (J) TIMP-1. Relative gene expression is relative to human GAPDH.
641 Error bars represent means \pm SEM. Significance was determined via the Kruskal-Wallis
642 test. *p<0.05.

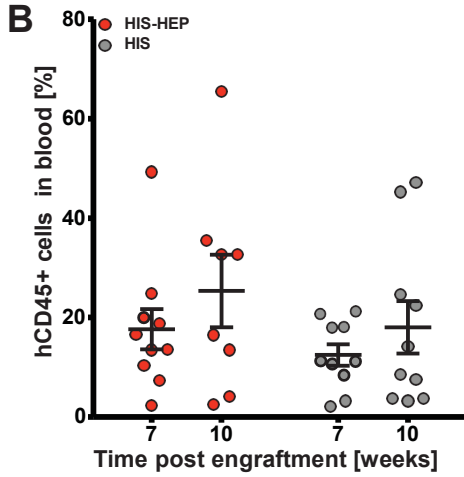
643

FIGURE 1

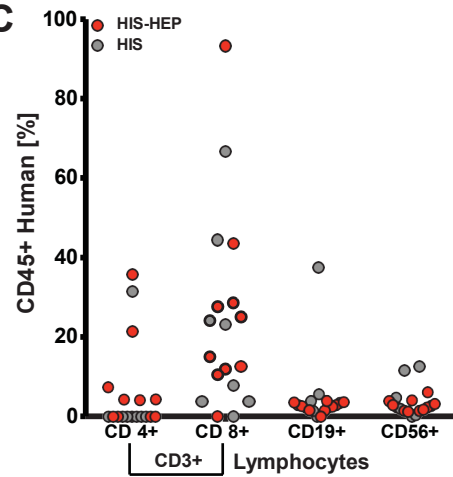
A



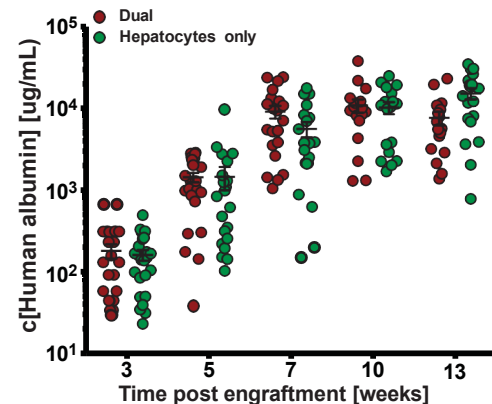
B



C



D



E

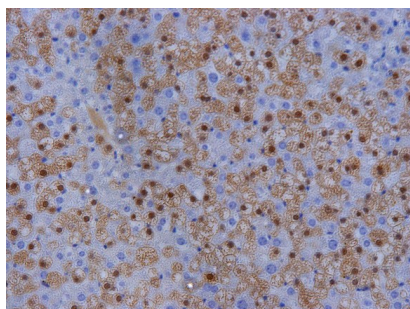


FIGURE 2

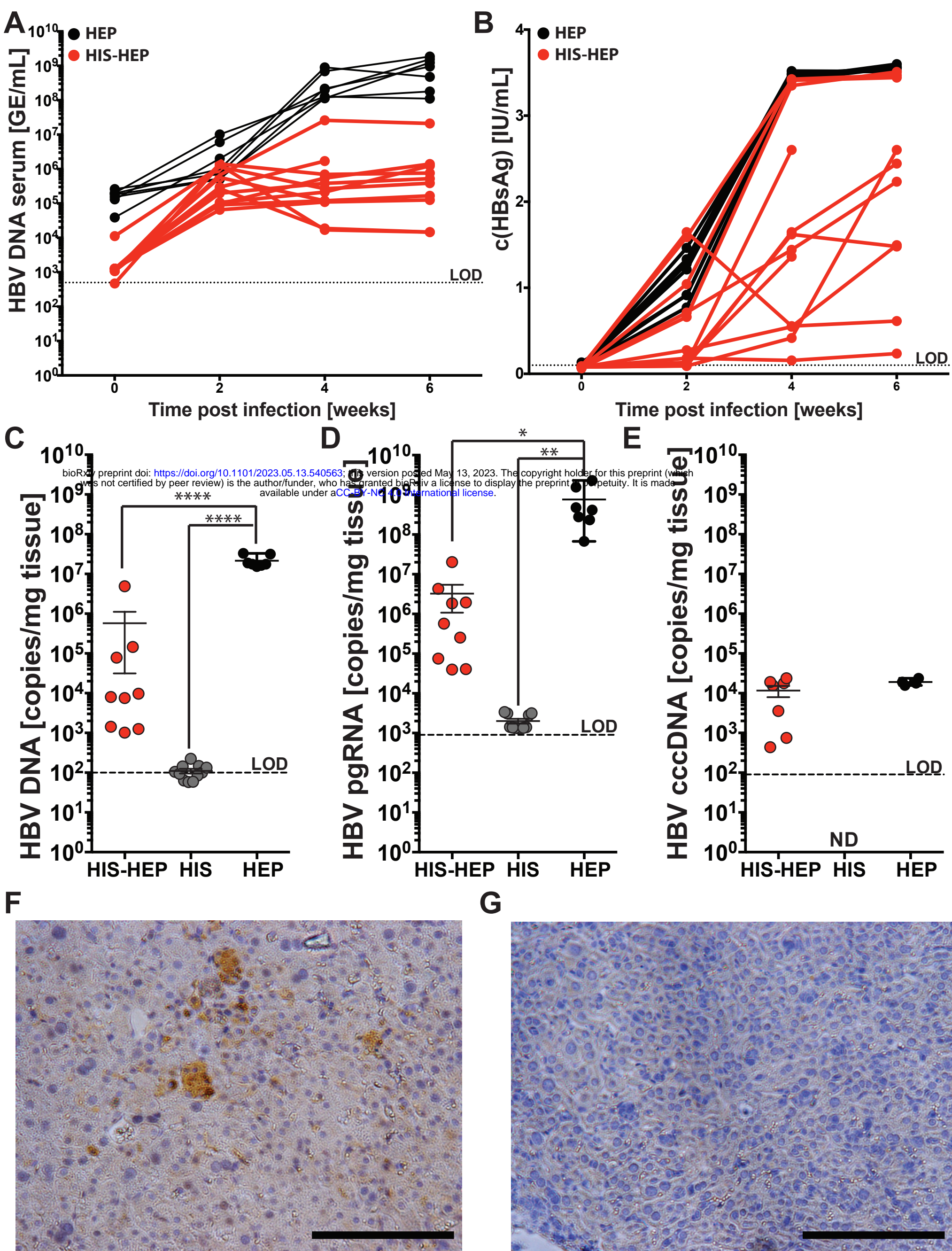


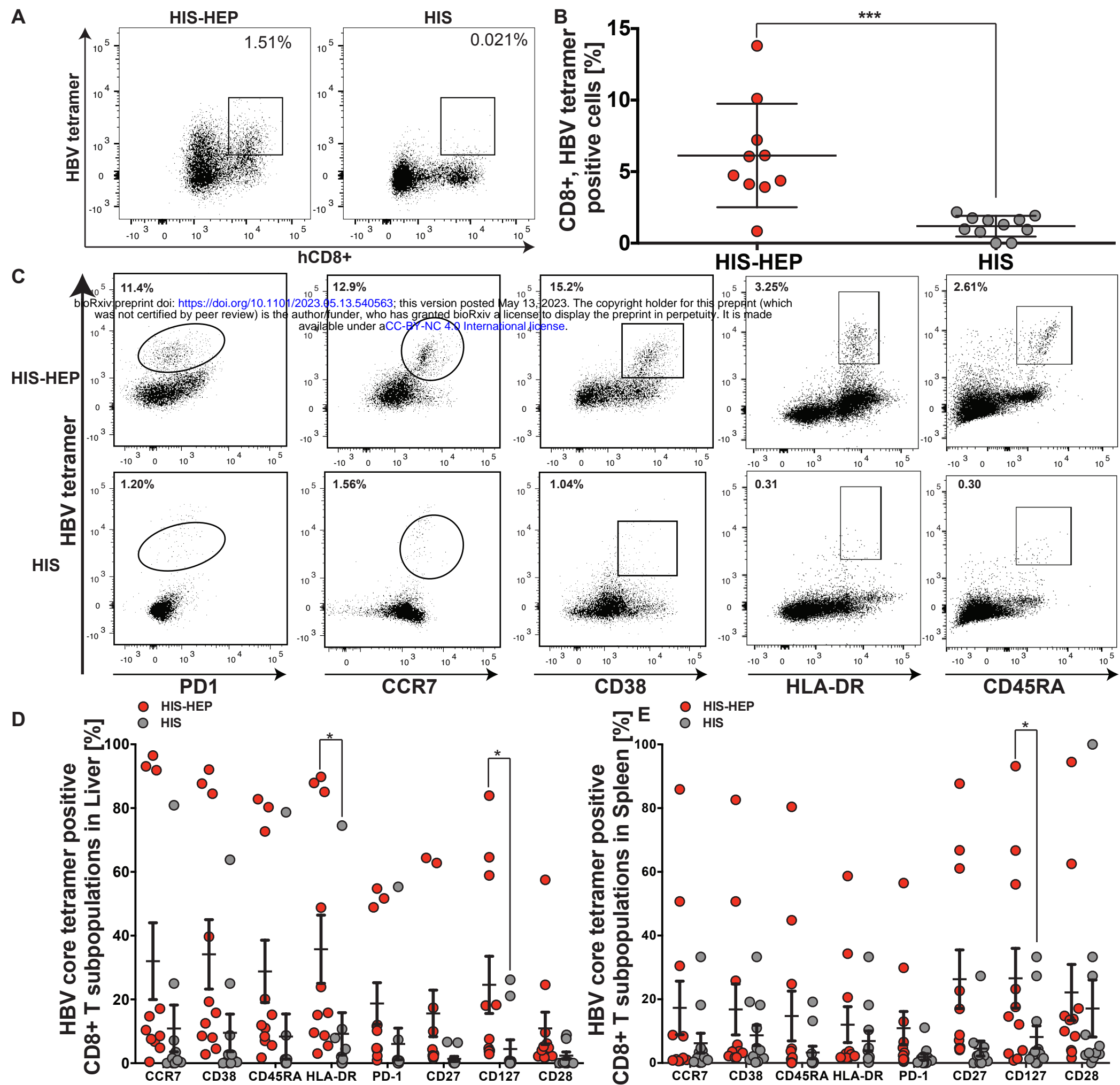
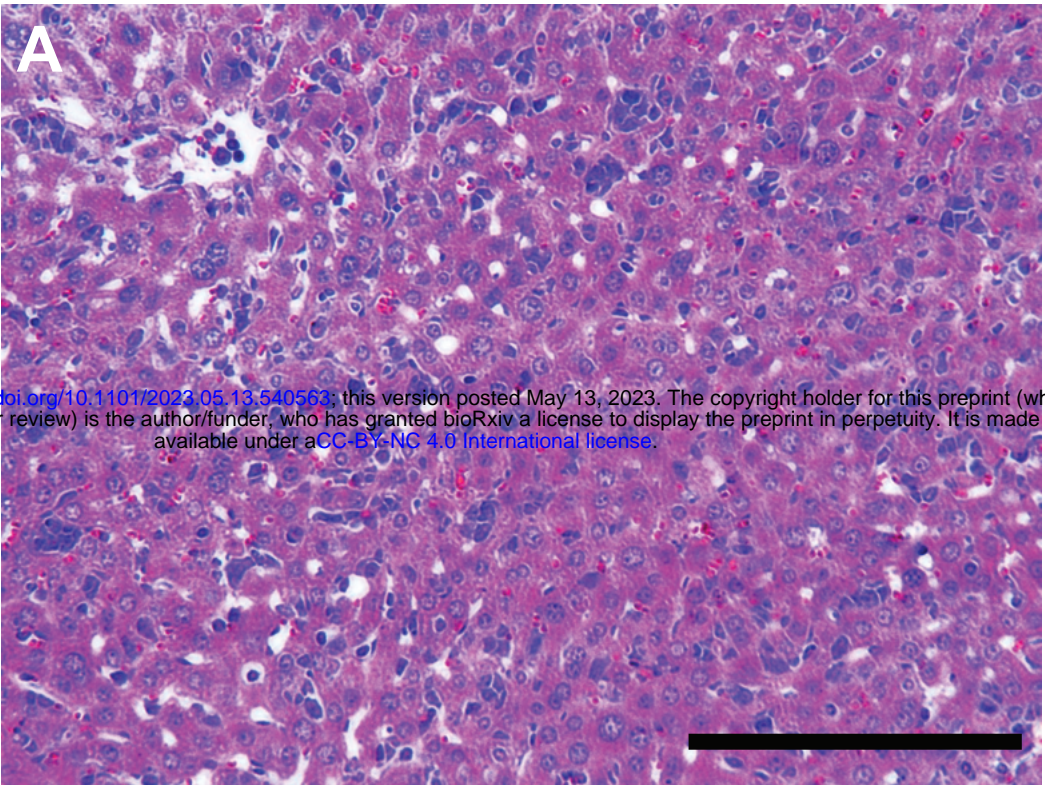
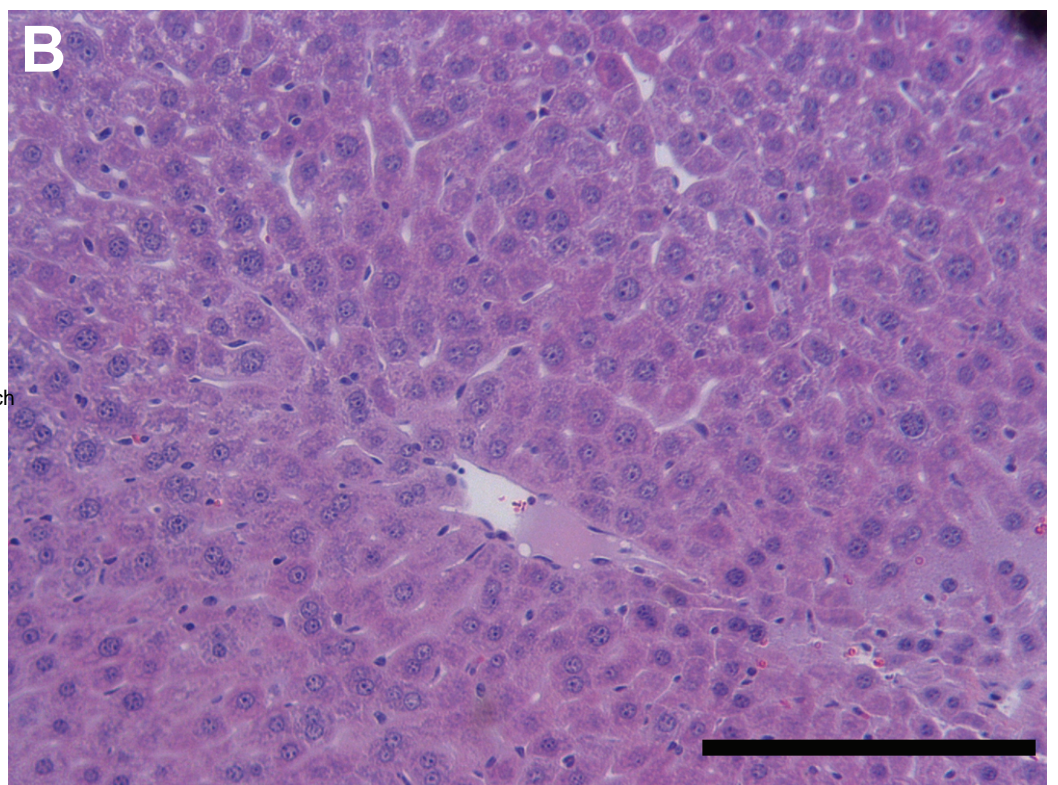
FIGURE 3

FIGURE 4

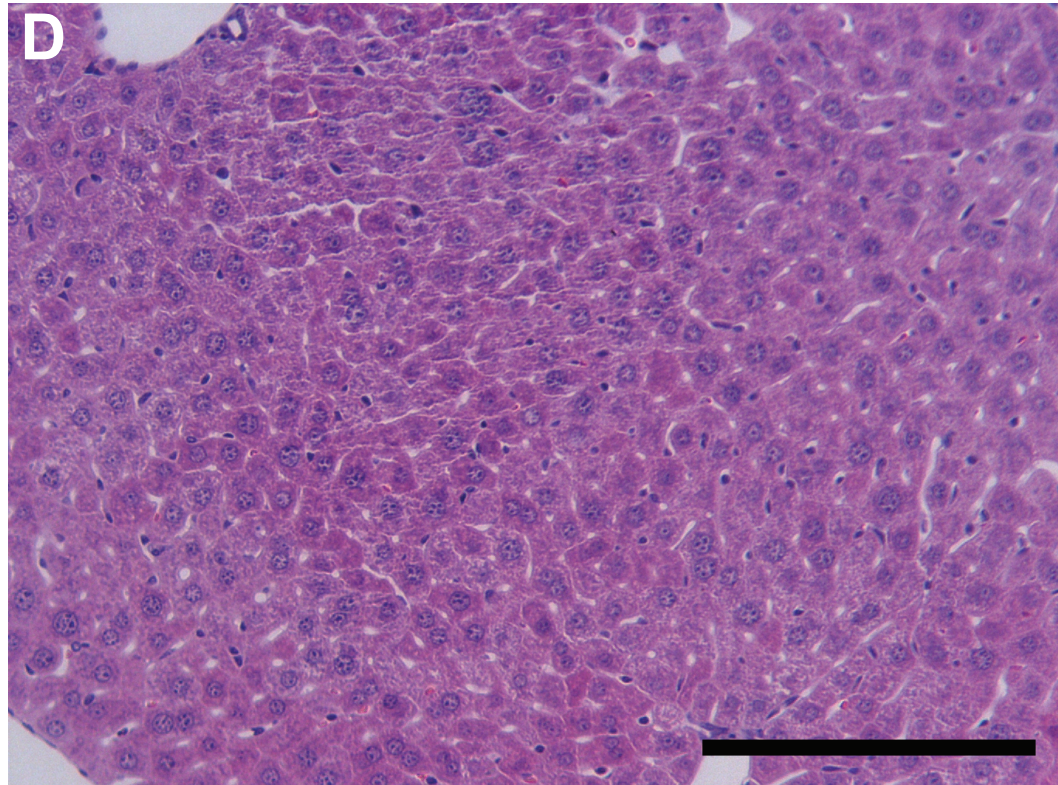
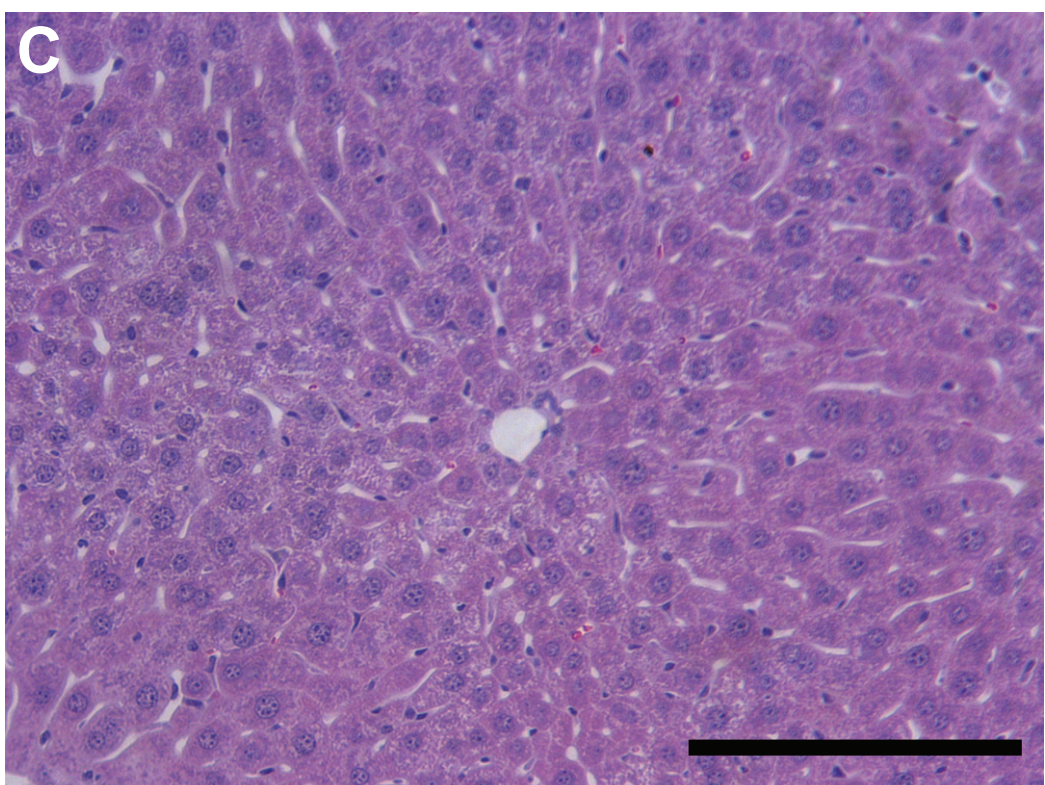
HBV-infected



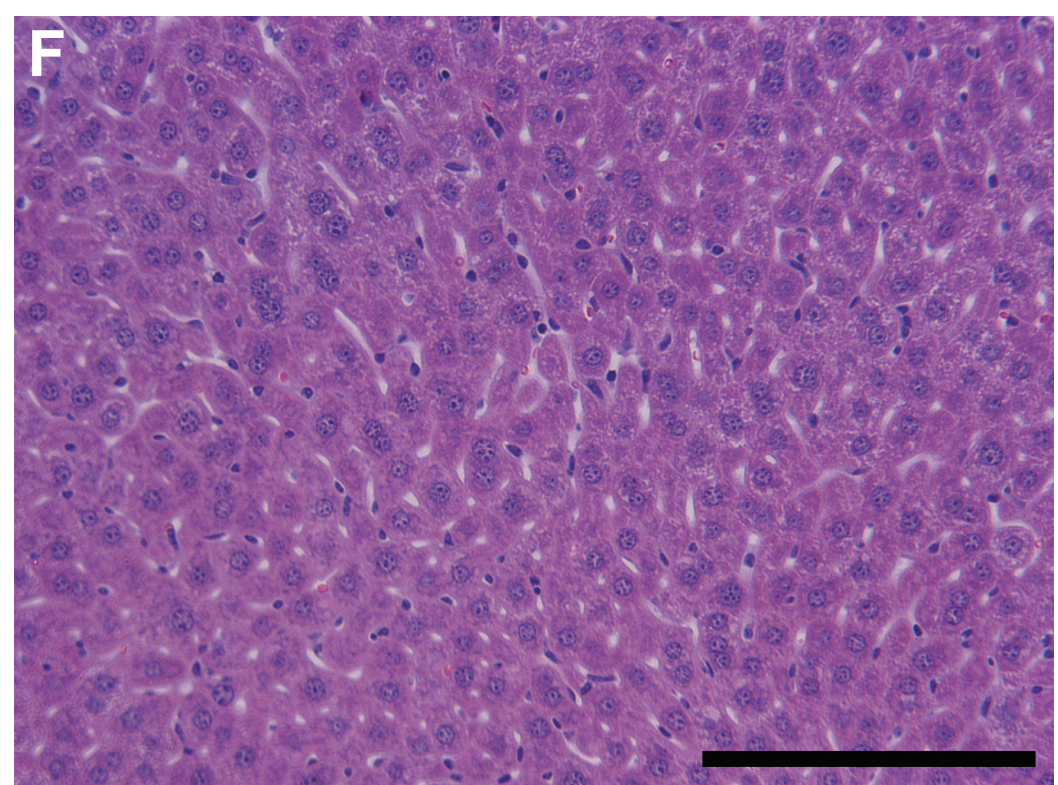
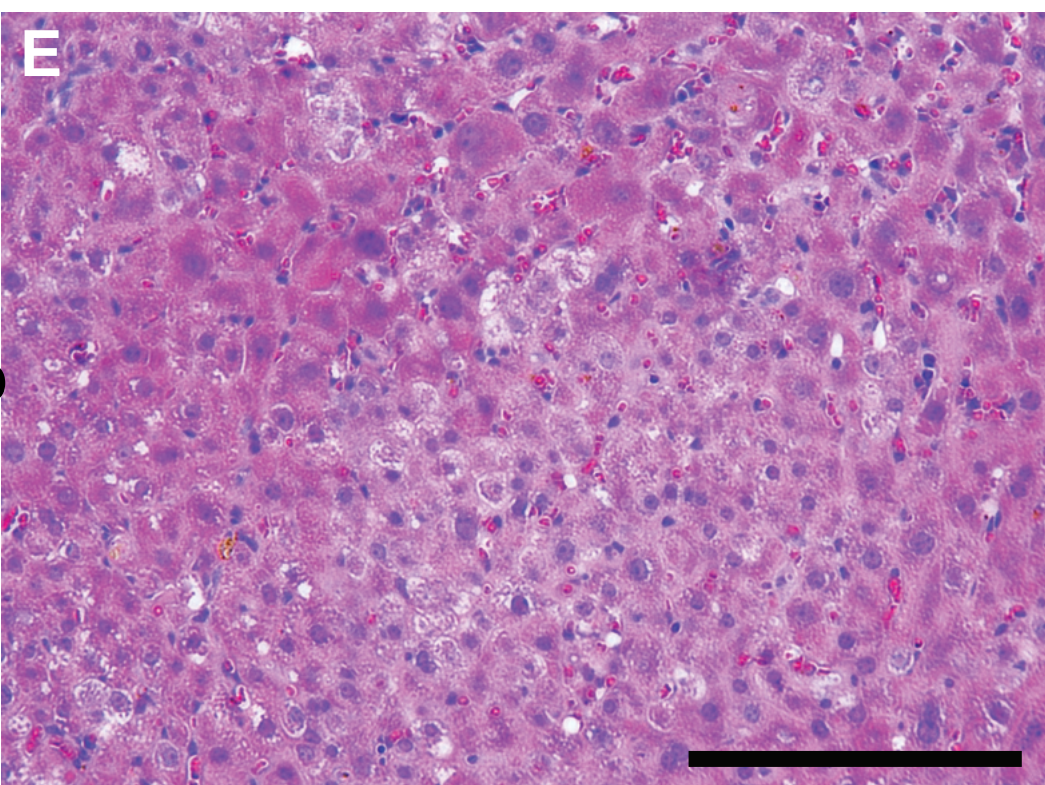
Non-infected



HEP



HIS-HEP



bioRxiv preprint doi: <https://doi.org/10.1101/2023.05.13.540563>; this version posted May 13, 2023. The copyright holder for this preprint (which was not certified by peer review) is the author/funder, who has granted bioRxiv a license to display the preprint in perpetuity. It is made available under aCC-BY-NC 4.0 International license.

FIGURE 5

A

NRGF/A2-hu HIS **Blood, liver, and spleen harvest**
bioRxiv preprint doi: <https://doi.org/10.1101/2023.05.13.540563>; this version posted May 13, 2023. The copyright holder for this preprint (which was not certified by peer review) is the author/funder, who has granted bioRxiv a license to display the preprint in perpetuity. It is made available under aCC-BY-NC 4.0 International license.

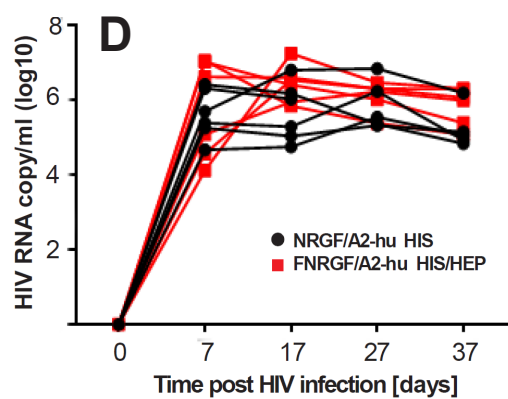
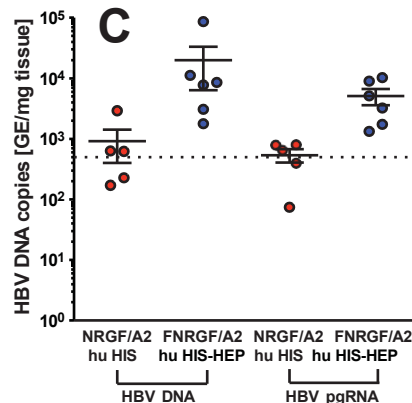
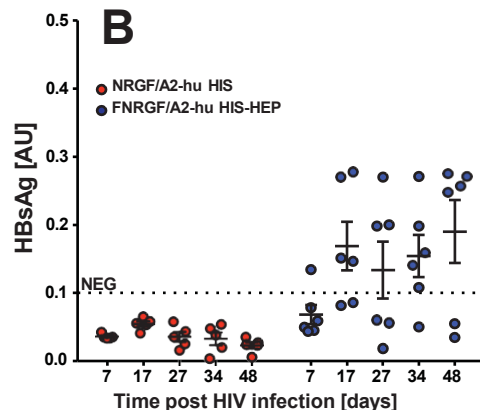
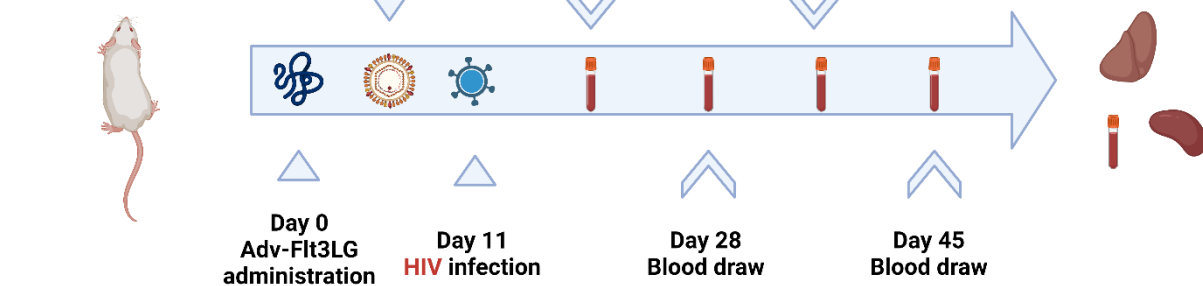
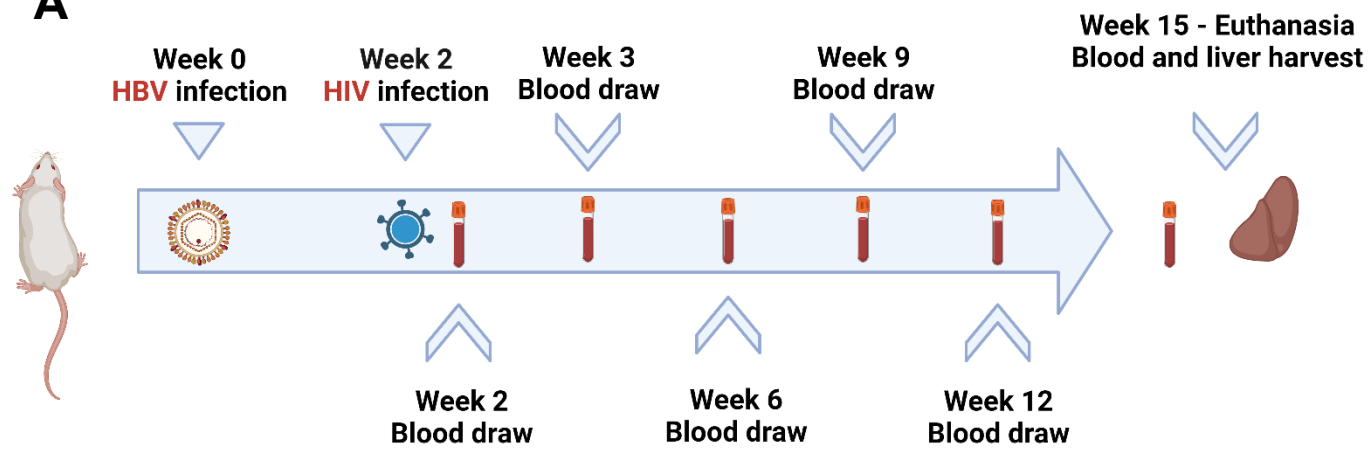
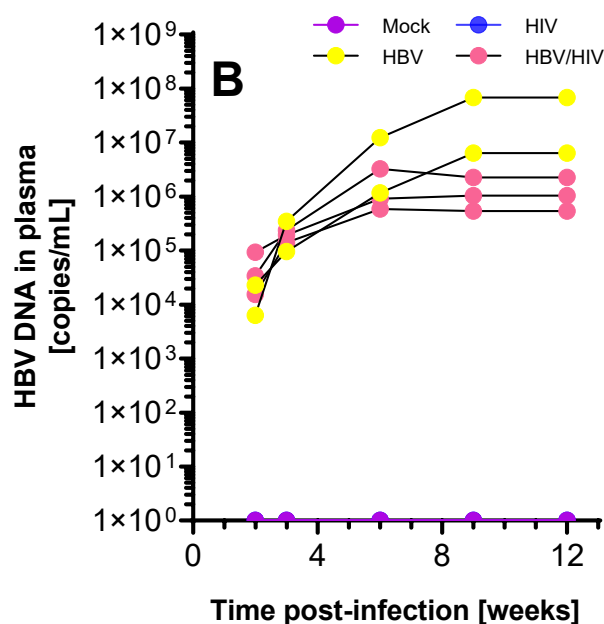


FIGURE 6

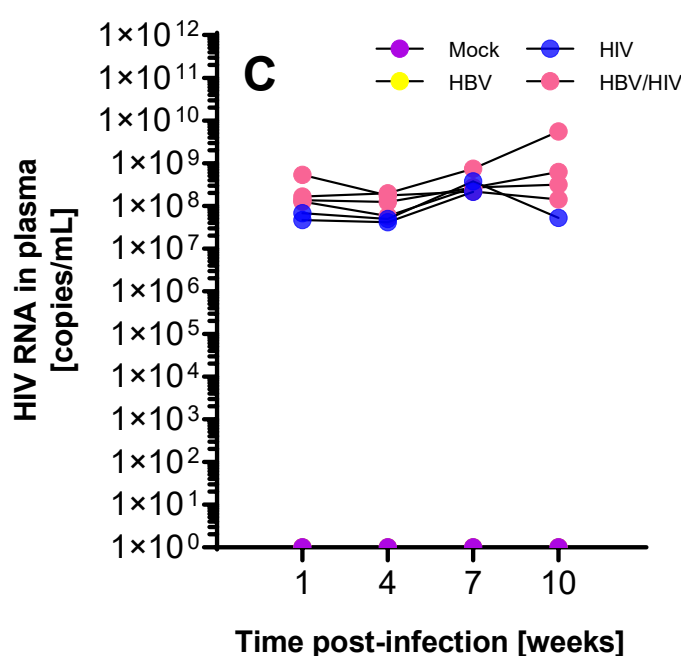
A



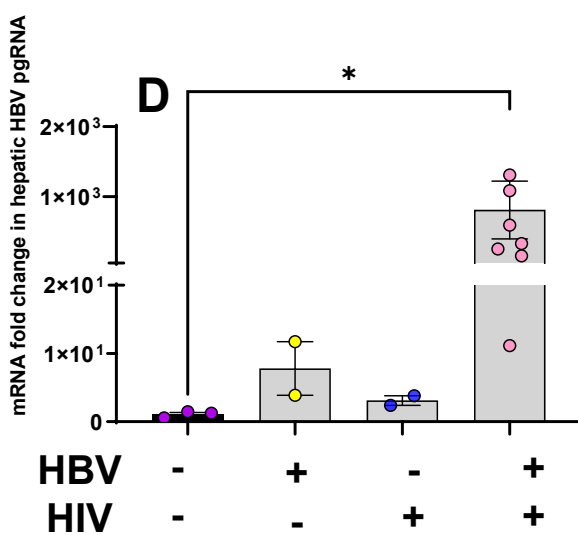
B



C



D



E

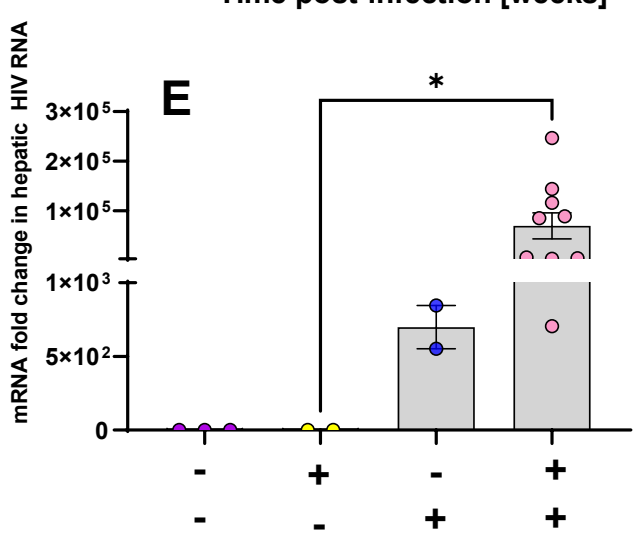
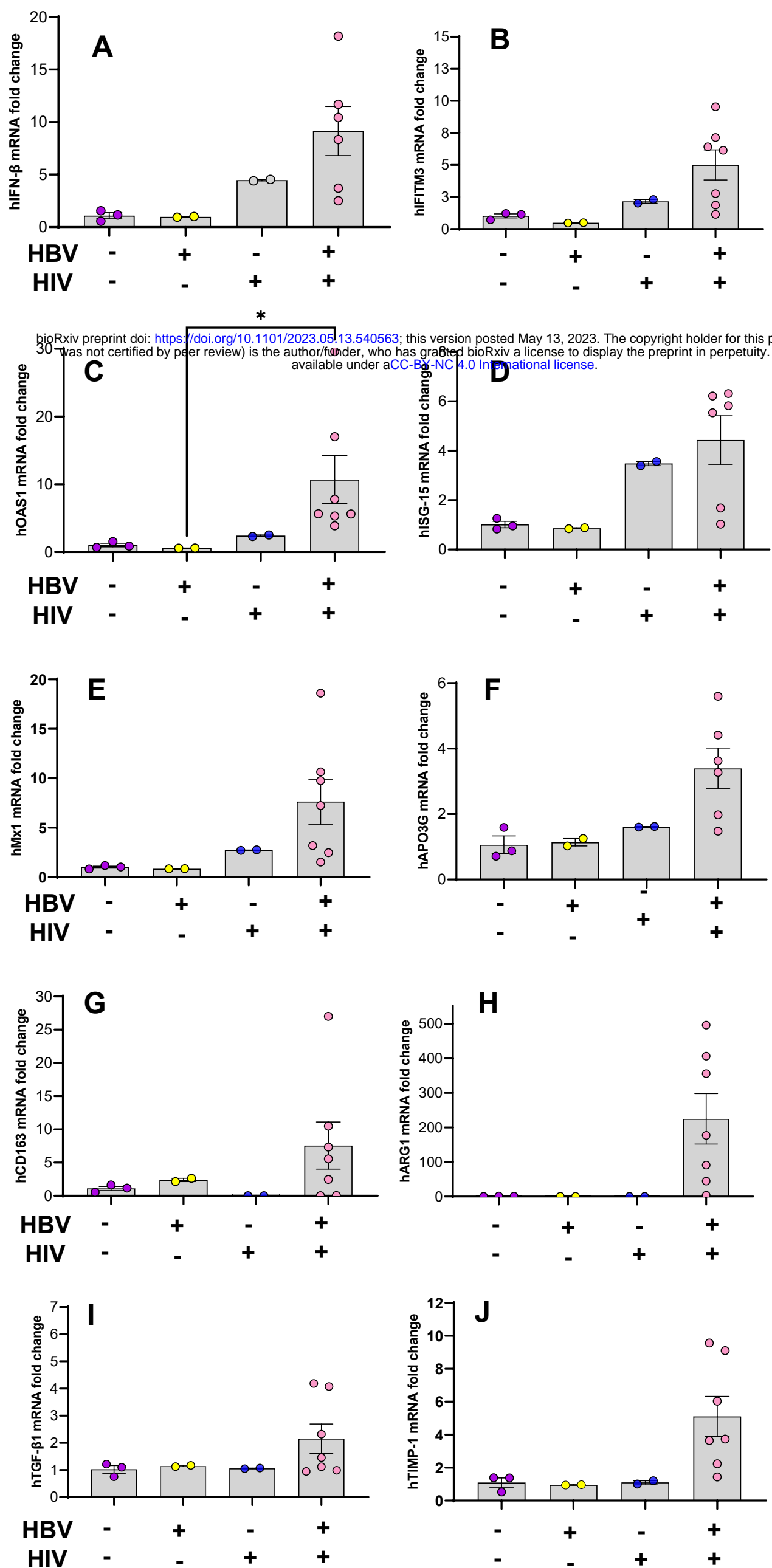


FIGURE 7



bioRxiv preprint doi: <https://doi.org/10.1101/2023.05.13.540563>; this version posted May 13, 2023. The copyright holder for this preprint (which was not certified by peer review) is the author/funder, who has granted bioRxiv a license to display the preprint in perpetuity. It is made available under aCC-BY-NC 4.0 International license.